

# Cystic Fibrosis Transmembrane Conductance Regulator Has an Altered Structure When Its Maturation Is Inhibited<sup>†</sup>

Eva Y.-J. Chen, M. Claire Bartlett, and David M. Clarke\*

Medical Research Council Group in Membrane Biology, Departments of Medicine and Biochemistry, University of Toronto, Toronto, Ontario, Canada M5S 1A8

Received November 12, 1999; Revised Manuscript Received January 13, 2000

**ABSTRACT:** Inefficient maturation and trafficking to the cell surface of the cystic fibrosis transmembrane conductance regulator (CFTR) is the primary cause of cystic fibrosis. CFTR protein that fails to mature accumulates as an immature core-glycosylated protein and is rapidly degraded. To determine how the structures of mature and immature CFTR are different, we compared the properties of CFTR that had been expressed in the presence or absence of the proteasome inhibitor, MG-132 (carbobenzoxy-L-leucyl-L-leucyl-L-leucinal). Transient expression of wild-type CFTR in the presence of submicromolar concentrations of MG-132 blocks maturation of the protein. We found that expression of CFTR in the presence of MG-132 trapped the protein in a trypsin-sensitive conformation. In addition, the structure of the carboxyl-terminus of immature and mature CFTR differed as histidine-tagged mature CFTR was preferentially recovered by metal-chelate chromatography. No chloride channel activity was detected when membranes containing immature CFTR were fused with planar lipid bilayers. These results show that expression of CFTR in the presence of MG-132 traps the protein in an altered conformation that may be inactive.

Cystic fibrosis (CF)<sup>†</sup> is a lethal genetic disease that is characterized by impaired epithelial salt and water transport. The disease is caused by mutations in the gene coding for the cystic fibrosis transmembrane conductance regulator (CFTR) (1). The protein is found on the apical surface of epithelial cells where it functions as a protein kinase A- and ATP-dependent chloride channel. In CF, impaired function of CFTR causes an alteration in the physical state of macromolecular secretions so that they cannot be cleared normally. The end result is the blockage of small diameter tubes, especially the small airways in the lung. The presence of excess mucus in the lungs leads to recurrent opportunistic infections that are the leading cause of death in CF (2).

Several hundred mutations have been identified in the CFTRs from patients with CF. The most common genetic

lesion (found in about 70% of patients) is deletion of phenylalanine 508 ( $\Delta$ F508). This mutation interferes in maturation of CFTR so that it is retained in the endoplasmic reticulum (ER) when expressed at normal physiological temperature.

We have systematically analyzed the effects of 30 other CF-associated mutations that are located in the intracellular loops of CFTR (3–5). We found that 18 of the mutants were defective in processing. Patients expressing these mutations had severe CF symptoms. The other 12 mutants were properly targeted to the cell surface and showed subtle changes in channel activity. Patients with these mutations had less severe symptoms.

These studies show that the majority of patients with severe CF symptoms express CFTR molecules that are defective in folding and intracellular trafficking. A potential strategy to treat patients expressing misprocessed CFTRs would be to induce the defective CFTRs to mature and migrate to the cell surface in a functional form. An important first step will be to understand the mechanisms required for maturation of CFTR.

Maturation of CFTR is inefficient. Only 20–40% of the wild-type protein synthesized reaches maturation and little, if any, of the misprocessed mutant CFTRs such as  $\Delta$ F508 reach maturation (6, 7). Maturation of some CFTR processing mutants such as  $\Delta$ F508 can, however, be induced by chemical chaperones (8, 9) or by expression at low temperature (10). The  $\Delta$ F508 mutant is functional when induced to the cell surface. It should be noted that induction of maturation of  $\Delta$ F508 by chemical chaperones or low temperature is very inefficient as less than 10% of the synthesized protein reaches the cell surface. An important

<sup>†</sup> This work was supported by grants from the Canadian Cystic Fibrosis Foundation, the Medical Research Council of Canada, and the National Institutes of Health (R01-CA80900). D.M.C. is a Scientist of the Medical Research Council of Canada and the Canadian Cystic Fibrosis Foundation Zellers Senior Scientist. E.Y.-J.C. is a recipient of the University of Toronto Open Scholarship.

\* Address correspondence to this author at the Department of Medicine, University of Toronto, Room 7342, Medical Sciences Building, 1 King's College Circle, Toronto, Ontario, Canada M5S 1A8. Tel 416-978-1105; Fax 416-978-1105; E-mail: david.clarke@utoronto.ca.

<sup>†</sup> Abbreviations: CF, cystic fibrosis; CFTR, cystic fibrosis transmembrane conductance regulator; Pgp, P-glycoprotein; MG-132, carbobenzoxy-L-leucyl-L-leucyl-L-leucinal; BFA, brefeldin A; SDS-PAGE, sodium dodecyl sulfate–polyacrylamide gel electrophoresis; endo F, endoglycosidase F; AEBSEF, 4-(2-aminoethyl)benzenesulfonfyl fluoride; TBS, Tris-buffered saline; PBS, phosphate-buffered saline; TPCK, L-1-tosylamido-2-phenylethyl chloromethyl ketone; PKA, cyclic AMP-dependent protein kinase; WT, wild type; ER, endoplasmic reticulum; ALLN, N-acetyl-L-leucyl-L-leucyl-L-norleucinal; E64, 1-[L-N-(trans-epoxysuccinyl)leucyl]amino-4-guanidinobutane.

goal in CF research is to understand the maturation process of CFTR in order to find ways of increasing the efficiency of maturation.

The objective of this paper was to compare the structures of mature and immature CFTRs. To block maturation and prevent degradation of immature CFTR, we carried out expression in the presence of MG-132, as we have previously shown MG-132 to block maturation of P-glycoprotein (11). MG-132 is a peptide aldehyde inhibitor designed to enter mammalian cells to inhibit the ubiquitin–proteasome pathway (12, 13). However, previous studies have shown that it also blocks maturation of CFTR (14). In this study, we compared the properties of mature CFTR to immature wild-type CFTR that accumulated in the presence of MG-132. Our results show that mature and immature CFTRs are structurally different and that immature CFTR may have little or no channel activity when its maturation is blocked by carrying out expression in the presence of MG-132.

## MATERIALS AND METHODS

**Construction of Mutants.** The CFTR point mutations were constructed and inserted into the mammalian expression vectors pcDNA3 or pMT21 as previously described (3, 5). For nickel-chelate chromatography, the full-length cDNA of WT and  $\Delta F508$  cDNA were modified to encode the epitope for monoclonal antibody A52 (15) and six histidine residues at the C-terminus. The sequence at the COOH terminus that would normally end in DTRL then became DTRRAIS-LISNSCSPEFDDLPLAEQREACRRGD(His)<sub>6</sub>PRQ.

**Expression of CFTR Wild Type and Mutants.** Subconfluent COS-1 or HEK 293 cells were transfected with the cDNA constructs with 1  $\mu$ g/mL of the various vector constructs using a calcium phosphate precipitation method adapted from Chen and Okayama (16). The medium was replaced with either plain medium or medium containing the appropriate concentrations of MG-132 (Biomol) or brefeldin A (BFA) (Alexis) at 15–20 h posttransfection. The cells were harvested after another 24–48 h.

**Endoglycosidase F Digestion.** CFTR WT cDNAs were expressed in COS-1 cells in 6-well plates. At 16 h posttransfection, the medium was replaced with either plain medium or medium containing 2  $\mu$ M MG-132. After incubation at 37 °C for another 24 h, the cells were solubilized with 2 $\times$  sample buffer with a protease inhibitor cocktail (3% SDS, 5%  $\beta$ -mercaptoethanol, 1 mM EDTA, 10% glycerol, 62.5 mM Tris-HCl, pH 6.8, 50  $\mu$ g/mL AEBSF [4-(2-aminoethyl)benzenesulfonyl fluoride], 10  $\mu$ g/mL aprotinin, 25  $\mu$ g/mL benzamidin, 1  $\mu$ g/mL E64, and 0.5  $\mu$ g/mL leupeptin). The samples were then divided into equal fractions and incubated with or without 500 units of endoglycosidase F (PNGase F; New England Biolabs) at 37 °C for 15 min. The samples were then subjected to SDS–PAGE and immunoblot analysis with mouse M3A7 monoclonal antibody (17) as the primary antibody and a horseradish peroxidase-labeled goat anti-mouse antibody as the secondary antibody. The signals were detected by chemiluminescence (enhanced chemiluminescence kit, Pierce).

**Isolation of Crude Membranes for Trypsin Digestion.** The crude membranes were prepared in the same manner as optimized by Loo and Clarke (18) for trypsin digestion assays. For each CFTR construct, 20 (100-mm) tissue culture plates of transfected HEK 293 cells were harvested and

washed with PBS (phosphate-buffered saline). The cell pellets were subsequently resuspended in 3 mL of low ionic strength buffer (10 mM Tris-HCl, pH 7.5, and 0.5 mM MgCl<sub>2</sub>). After incubation on ice for 10 min to allow the cells to swell, the samples were homogenized by 40 strokes in a loose-fitting Dounce homogenizer, followed by 20 strokes after addition of 3 mL of sucrose buffer (10 mM Tris-HCl, pH 7.5, 500 mM sucrose, and 0.3 M KCl). The cell debris was removed by centrifugation at 3000g for 7 min at 4 °C. The crude membranes were collected from the supernatant by centrifugation at 44000g for 45 min at 4 °C and resuspended with 300  $\mu$ L of TBS (Tris-buffered saline; 10 mM Tris-HCl, pH 7.5, and 150 mM NaCl). The crude membranes were immediately used for the trypsin digestion.

**Trypsin Digestion.** Crude membranes from various constructs were treated with different concentrations of TPCK-trypsin (L-1-tosylamido-2-phenylethyl chloromethyl ketone-treated trypsin; Sigma, 12 000 BAEE units/mg) at room temperature for 5 min; the final concentrations of TPCK-trypsin were 0, 0.1, 1, 10, 100, and 1000  $\mu$ g/mL. The reactions were stopped by the addition of 2 mg/mL lima bean trypsin inhibitor (Worthington). The crude membranes were then solubilized with 2 $\times$  sample buffer (3% SDS, 5%  $\beta$ -mercaptoethanol, 10% glycerol, and 62.5 mM Tris-HCl, pH 6.8), subjected to separation by SDS–PAGE (19), and analyzed by Western blot with monoclonal antibody M3A7 as described above.

**Nickel-Chelate Chromatography.** The purification scheme by Ni-chelate chromatography used by Loo and Clarke (20) was adopted for use with the multihistidine-tagged CFTR constructs. The protocol was not efficient for the recovery of histidine-tagged CFTR (see Results) but was useful for comparison of mature and immature CFTR. For each CFTR construct, 20 (100-mm) tissue culture plates of transfected COS-1 cells were harvested and washed with PBS. The cell pellets were resuspended in 650  $\mu$ L of resuspension buffer [50 mM NaPO<sub>4</sub>, pH 8.0, 150 mM NaCl, and 20% (v/v) glycerol] and solubilized by the addition of 750  $\mu$ L of solubilization buffer [50 mM NaPO<sub>4</sub>, pH 8.0, 150 mM NaCl, 2% (w/v) *n*-dodecyl  $\beta$ -D-maltoside, 20% (v/v) glycerol, 50  $\mu$ g/mL AEBSF, 10  $\mu$ g/mL aprotinin, 25  $\mu$ g/mL benzamidin, 1  $\mu$ g/mL E64, and 0.5  $\mu$ g/mL leupeptin]. Insoluble material was removed by centrifugation at 16000g for 5 min. NaCl and imidazole (pH 7.0) were added to 1.3 mL of the subsequent supernatant to make final concentrations of 300 mM NaCl and 6.8 mM imidazole. The supernatant was then incubated with 50  $\mu$ L of 50% (w/v) suspended Ni–NTA Superflow resin (Qiagen) overnight at 4 °C with mixing. The resins were collected by centrifugation at 16000g for 2 min. The resin was washed twice with 500  $\mu$ L of wash buffer [10 mM Tris-HCl, pH 7.5, 500 mM NaCl, 50 mM imidazole, 0.1% (w/v) *n*-dodecyl  $\beta$ -D-maltoside, 20% and (v/v) glycerol] by resuspension and centrifugation. The proteins were eluted with 60  $\mu$ L of elution buffer [10 mM Tris-HCl, pH 7.5, 500 mM NaCl, 333 mM imidazole, 0.1% (w/v) *n*-dodecyl  $\beta$ -D-maltoside, and 20% (v/v) glycerol]. Finally, 100  $\mu$ L of 500 mM EDTA (chelator of nickel) was added to the resin to elute any remaining protein. Fractions from each step were collected and equivalent amounts of sample were analyzed by SDS–PAGE and followed by immunoblot analysis as described above but with mouse monoclonal antibody A52 as the primary antibody.

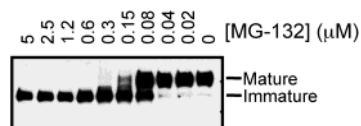


**FIGURE 1: Effect of MG-132 on expression of CFTR.** COS-1 cells transiently transfected with wild-type CFTR cDNA were treated with the indicated concentrations of MG-132. Whole-cell extracts were subjected to SDS-PAGE and immunoblot analysis as described under Materials and Methods.

**Isolation of Crude Membranes for Planar Lipid Bilayer Studies.** For the planar lipid bilayer studies, the crude membranes were prepared as optimized by Tao et al. (21). For each CFTR construct, 10 (100-mm) tissue culture plates of transfected HEK 293 cells were harvested and washed with ice-cold PBS. The cell pellets were subsequently resuspended in 4 mL of ice-cold hypotonic lysis buffer (10 mM HEPES, pH 7.2, 1 mM EDTA, 50  $\mu$ g/mL AEBSF, 10  $\mu$ g/mL aprotinin, 25  $\mu$ g/mL benzamidine, 1  $\mu$ g/mL E64, and 0.5  $\mu$ g/mL leupeptin). After incubation on ice for 5 min to allow the cells to swell, the samples were lysed by 10 strokes in a loose-fitting Dounce homogenizer, followed by 15 strokes after addition of 4 mL of sucrose buffer (500 mM sucrose and 10 mM HEPES, pH 7.2). The cell debris was pelleted and removed by centrifugation at 3000g for 7 min at 4 °C. The crude membranes were pelleted from the supernatant by centrifugation at 110000g for 1 h at 4 °C and resuspended with 200  $\mu$ L of prephosphorylation buffer (250 mM sucrose, 10 mM HEPES, pH 7.2, and 5 mM Mg-ATP). The crude membranes were stored at -70 °C in 20  $\mu$ L aliquots until use. The total protein concentrations were measured with the BCA protein assay kit from Pierce.

**Planar Lipid Bilayer Reconstitution of CFTR Channels.** Brain L- $\alpha$ -phosphatidylethanolamine and brain L- $\alpha$ -phosphatidylserine (Avanti Polar Lipids Inc.) dissolved in chloroform were mixed in 5:3 (w/w) ratio and dried under nitrogen gas. The lipid mix was dissolved in *n*-decane to make a total lipid concentration of 35 mg/mL. Bilayers were formed across a 300  $\mu$ m aperture in a delrin partition separating two chambers. The cis chamber (400  $\mu$ L), where the crude membranes are added, was connected to the headstage input of a model EPC-7 amplifier (List-Electronics, Darmstadt, Germany). The trans (1.2 mL) chamber was held at virtual ground. During recording, the trans chamber was filled with recording solution containing 250 mM KCl and 10 mM HEPES (pH 7.6). The cis chamber was filled with the same recording solution with additions of 0.1 mM MgCl<sub>2</sub>, 4 mM Mg-ATP, 40 casein units of PKA, and 5–30  $\mu$ g of the respective crude membranes. During the recording, the cis chamber, which corresponds to the cytoplasmic side of the CFTR protein, was held at -80 mV. The recordings were filtered at 10 000 Hz, digitized at 44.1 kHz (PCM-2 A/D VCR adapter; Medical Systems Corp., Greenvale, NY) and recorded on VHS videotapes. Upon playback, the data were filtered at 100 Hz and acquired with pClamp 5.5 (Axon Instruments) at a sampling rate of 2000  $\mu$ s.

## RESULTS

Figure 1 shows that the major product of wild-type CFTR cDNA expressed in COS-1 cells in the absence of MG-132 is the mature 170 kDa product. To compare the properties of immature and mature forms of CFTR, we first needed to

express immature CFTR alone. A method that blocks maturation of CFTR is to express the cDNA in the presence of MG-132 (14, 22).

To determine the optimal concentration of MG-132 for blocking CFTR maturation, expression of CFTR cDNA was carried out using the pcDNA3 vector and COS-1 cells because this expression system yields relatively high levels of mature CFTR protein. Transiently transfected COS-1 cells were treated for 2 days with concentrations of MG-132 ranging from 0.02 to 5  $\mu$ M MG-132 (Figure 1) at 20 h posttransfection. The two N-glycosylation sites on the putative extracellular loop 4 of CFTR enables us to determine the maturation state of the protein. Although the core glycosylation occurs in the ER (endoplasmic reticulum), the carbohydrate is modified only if it has progressed into the medial Golgi. The modification of the carbohydrate moiety leads to a shift in the protein's apparent molecular mass: the core-glycosylated immature protein has an apparent molecular mass of ~140 kDa, while the fully glycosylated mature CFTR has an apparent molecular mass of ~170 kDa.

Increased levels of immature CFTR were observed in the presence of 0.08  $\mu$ M MG-132 and there was a dramatic decrease in level of the mature protein at a concentration of 0.15  $\mu$ M MG-132. No mature protein could be detected for samples treated with 0.3  $\mu$ M MG-132 or higher amounts of MG-132. Figure 1 shows that maturation of WT CFTR in cells may be completely blocked by 0.3  $\mu$ M MG-132 or more. For the remainder of the study, we used 2  $\mu$ M MG-132 to block maturation of CFTR.

In a recent report by Johnston et al. (23), they reported the discovery of a novel cytosolic entity, the aggresome, which they proposed to have formed in the presence of a protease inhibitor, *N*-acetyl-L-leucyl-L-leucyl-L-norleucinal (ALLN). They proposed the aggresome to be a cellular response to accumulated membrane proteins in the ER. In the presence of ALLN, ER-accumulated membrane proteins such as CFTR translocate across the ER membrane into the cytosol and accumulate into detergent-insoluble aggregates to form the aggresome. CFTR that accumulates in aggresomes can be distinguished from CFTR in the ER because it has been deglycosylated.

To determine whether the CFTR protein accumulated in the presence of MG-132 remains in the ER membrane, we subjected the proteins to endoglycosidase F (endo F) digestion (Figure 2). Endo F completely removes all sugar residues from N-glycosylated proteins. The rationale was that if the accumulated product has been transported to the cytosol by retrotranslocation (24, 25), then the glycosidases in the cytosol would have already removed the carbohydrate. However, if the protein remains in the ER membrane, we would expect to see a shift in molecular mass when the protein is treated with endo F. In Figure 2, we see efficient endo F cleavage of the sugars on wild-type (WT) CFTR. The shift is also observed in the MG-132-treated WT CFTR. This suggests that MG-132 traps WT CFTR in the ER membrane. Similar shifts were observed in  $\Delta$ F508 CFTR (Figure 2). Both untreated  $\Delta$ F508 and MG-132-treated  $\Delta$ F508 showed shifts in apparent molecular mass when treated with endo F. We repeated the endoglycosidase digestion on normally expressed and MG-132-treated P-glycoprotein (Pgp) (Figure 2), CFTR's sister protein, and similar results were observed. Pgp is an ABC drug transporter



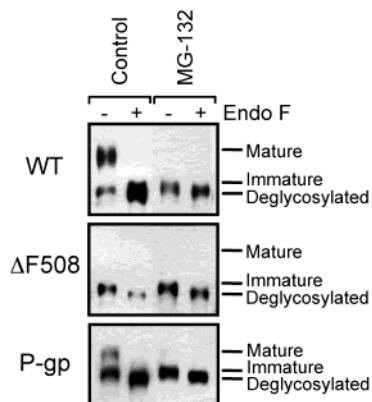


**FIGURE 2: Endoglycosidase F digestion.** COS-1 cells expressing wild-type CFTR, mutant  $\Delta F508$ , or P-glycoprotein were treated with (MG-132) or without (control)  $2 \mu\text{M}$  MG-132. Whole-cell extracts were subsequently treated with (+) or without (–) endoglycosidase F (Endo F). The samples were separated by SDS–PAGE (5.5%) followed by immunoblot analysis. The mature, immature, and deglycosylated protein bands are indicated.

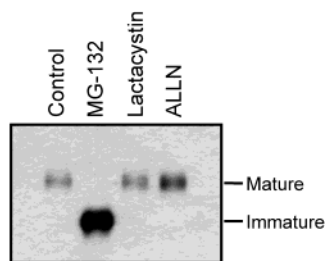


**FIGURE 3: Effect of protease inhibitors on CFTR maturation.** COS-1 cells transiently transfected with WT CFTR cDNA were treated with no protease inhibitors (control),  $2 \mu\text{M}$  MG-132,  $2 \mu\text{M}$  lactacystin, or  $2 \mu\text{M}$  *N*-acetyl-L-leucyl-L-leucyl-L-norleucinal (ALLN). The cells were subsequently lysed and subjected to immunoblot analysis (monoclonal antibody M3A7).

that is responsible for the multidrug resistance phenomenon in cancer chemotherapy. Its maturation is also blocked by MG-132 (11). This indicates that MG-132 has the same action on membrane proteins such as CFTR and Pgp.

We also examined the effects of other protease inhibitors on the maturation of CFTR (Figure 3). Thus, in addition to treating transiently transfected COS-1 cells with  $2 \mu\text{M}$  MG-132, we also incubated them with  $2 \mu\text{M}$  lactacystin or  $2 \mu\text{M}$  ALLN. Both lactacystin and ALLN are potent inhibitors of the 20S proteasome. As shown in Figure 3, only MG-132 was able to completely block maturation of CFTR. Lactacystin and ALLN had no apparent effect on CFTR maturation in COS-1 cells.

Next, we compared the structures of mature and immature CFTR by looking at their sensitivity to trypsin digestion. Our rationale was that if there were differences in structure, then exposure of trypsin-sensitive sites would differ, leading to variations in trypsin sensitivity. The  $\Delta F508$  processing mutant was included to test whether its trypsin sensitivity resembled that of mature or immature WT protein. Crude membranes made from COS-1 cells transfected with WT, MG-132-treated WT, and  $\Delta F508$  CFTR were incubated with various amounts of trypsin for 5 min. The reactions were then stopped with the addition of lima bean trypsin inhibitor. Figure 4 shows that WT mature CFTR is quite resistant to trypsin. It takes  $1000 \mu\text{g/mL}$  trypsin for it to be completely digested (Figure 4). Both immature CFTR from MG-132-

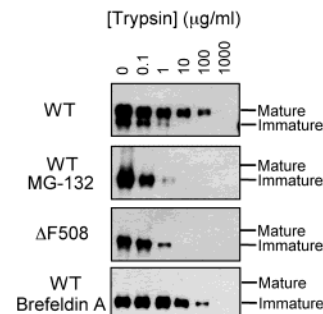


**FIGURE 4: Trypsin sensitivity of CFTR.** Membranes were prepared from COS-1 cells transiently transfected with wild-type (WT) CFTR cDNA, wild type treated with  $2 \mu\text{M}$  MG-132 (WT MG-132),  $\Delta F508$  CFTR cDNA, or wild type treated with  $10 \mu\text{g/mL}$  brefeldin A. The membranes were treated with various concentrations (0–1000  $\mu\text{g/mL}$ ) of TPCK-treated trypsin. The reactions were stopped by the addition of lima bean trypsin inhibitor. Equivalent amounts of protein were subjected to immunoblot analysis (monoclonal antibody M3A7).

treated WT and  $\Delta F508$  show much more sensitivity to trypsin digestion. Immature WT CFTR or  $\Delta F508$  were digested after treatment with only 1–10  $\mu\text{g/mL}$  trypsin.

The immature CFTR's 100–1000-fold increase in trypsin sensitivity suggests that it may be more loosely folded than mature CFTR. However, there is also the possibility that the observed difference in trypsin sensitivity is due to differences in the subcellular location or the glycosylation state of the two species of CFTR protein. The differences in lipid environment and carbohydrate moiety might provide hindrance to trypsin action to CFTR proteins in the plasma membrane. To block trafficking of CFTR to the plasma membrane and the addition of complex carbohydrate in the Golgi, expression was carried out in the presence of brefeldin A (BFA). BFA is known to inhibit the trafficking of CFTR out of the ER without blocking CFTR protein maturation (26). As shown in Figure 4, BFA-treated WT CFTR exhibits similar trypsin sensitivity as the plasma membrane-localized WT CFTR. This shows that neither the subcellular location nor the glycosylation state of CFTR has a significant effect on its trypsin sensitivity. Thus, the variation in trypsin sensitivity of mature and immature CFTR protein is likely to be due to their structural differences.

The structural differences between the two forms of CFTR are further evident in an observation made during our attempt to purify histidine-tagged CFTR by nickel chelate chromatography. Full-length WT CFTR cDNA was modified to include a six-histidine tag at its C-terminus. An A52 epitope tag was also added at the C-terminus, in front of the histidine tag, to evaluate the intactness of the C-terminus over the purification process. The CFTR protein was expressed in COS-1 cells and harvested for purification. The harvested cells were first solubilized with the detergent dodecyl maltoside. Sodium chloride and imidazole were added to the solubilized samples to minimize other proteins' nonspecific interaction with the CFTR protein and the nickel resin. After overnight incubation with nickel-based affinity resin at  $4^\circ\text{C}$ , the unbound proteins were removed from the resin. The nickel resin was then washed several times with a wash buffer containing a low concentration of imidazole (50 mM) to remove other weakly bound proteins. The histidine-tagged CFTR protein was then eluted with a buffer containing a high concentration of imidazole (333 mM).

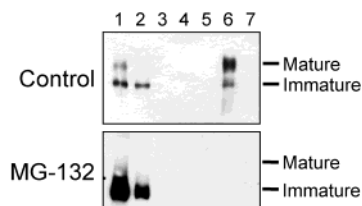


**FIGURE 5: Purification profiles of WT CFTR.** COS-1 cells were transiently transfected with modified WT CFTR cDNA with the C-terminus modified to include an A52 epitope and a six-histidine tag. One batch of cells was treated with 2  $\mu$ M MG-132 at 20 h posttransfection (MG-132), while the control just had its medium replaced (control). The cells were harvested and subjected to nickel affinity chromatography. Samples were taken from each step and analyzed by immunoblotting (monoclonal antibody A52): Lanes 1, total solubilized; lanes 2, unbound; lanes 3, wash 1; lanes 4, wash 2; lanes 5, eluted (equivalent amount to total solubilized); lanes 6, concentrated eluted; lanes 7, EDTA-eluted.

Figure 5 shows the purification profiles of wild-type CFTR (control) and MG-132-treated wild-type CFTR. In both panels, lanes 1 show the total level of expression of CFTR in COS-1 cells. Lanes 2 show the CFTR not bound to the resin. In the WT control, virtually all of the mature CFTR was bound to the nickel resin while the immature CFTR binds less efficiently (Figure 5, lanes 2). Lanes 3 and 4 show the amount of CFTR present in the washes; only upon overexposure of the blot could small amounts of CFTR be detected in the washes. Equivalent amounts of the eluted samples (as compared to that of the total sample) were loaded in lanes 5 of both panels, while more concentrated samples were loaded in lanes 6. The failure to detect CFTR protein in lanes 5 indicates a low yield of the purification protocol. To ensure that all protein bound to the nickel has been accounted for, the remainder protein was eluted with 500 mM EDTA. EDTA is a chelator of nickel. Elution with EDTA should show how much protein was left bound to the nickel. From the immunoblots, the majority of CFTR has been either eluted or gradually digested over the course of purification. Furthermore, elution of the resin with SDS, which denatures the protein present in the resin, indicated that some of the protein was bound to the physical support of the resin (data not shown).

The results in Figure 5 show that mature CFTR interacts much more efficiently with the nickel resin than immature CFTR. In the solubilized control sample, there was more protein in the immature form than in the mature form. In the eluted sample, however, there was more protein in the mature form than in the immature form; the intensities of the mature and immature bands are reversed in the eluted samples. Again, this observation suggests structural differences in the two forms of the CFTR protein.

Next, we examined the functionality of the immature wild-type CFTR protein trapped by expression in the presence of MG-132 (Figure 6). To do this, we took crude membranes made from MG-132-treated CFTR-expressing HEK 293 cells and incorporated CFTR into planar lipid bilayer to look for channel activity. HEK 293 cells were used because they provide higher expression. After many trials, no channel activity could be observed for the ER-trapped immature wild-type CFTR. However, we could always detect channel activity from the control wild-type samples. We then examined the functionality of  $\Delta$ F508, which has no detectable mature CFTR protein on an immunoblot. No channel

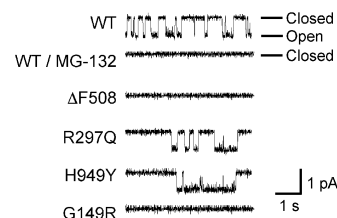


**FIGURE 6: Channel activity of CFTR variants.** Membranes were prepared from HEK cells transiently transfected with various CFTR cDNAs: WT,  $\Delta$ F508, R297Q, H949Y, and G149R. In addition, one batch of WT cells was treated with 2  $\mu$ M MG-132. PKA-stimulated channel activity was analyzed after incorporation into lipid bilayers at  $-80$  mV under isotonic conditions. The recording solution contained 250 mM KCl and 10 mM HEPES (pH 7.6).

activity could be detected. We then assayed three other mutants that expressed different levels of mature CFTR. R297Q, which shows a similar level of maturation as the wild-type CFTR, showed CFTR-like channel activity. H949Y is a partially processing-defective mutant that expressed less than 10% of the mature band, relative to wild type (3). It, too, exhibited CFTR-like channel activity. G149R, like  $\Delta$ F508, is a processing mutant with no detectable mature CFTR protein. In this case, no channel activity was detected. This suggests immature CFTR is not functional, possibly because it has not yet properly folded.

## DISCUSSION

Maturation of CFTR after synthesis is a particularly relevant process in devising strategies to treat CF since most CF patients express CFTRs that are defective in processing. Our results suggest that mature CFTR is structurally quite different from immature CFTR. The trypsin results clearly show a difference in trypsin sensitivity between mature and immature CFTR. This suggests differences in the folding of the two forms of CFTR. The low affinity of immature histidine-tagged CFTR with nickel resin also suggests differences in the folding of the two forms at the C-terminus since the histidine tag was placed at the C-terminus of the protein. These results strongly suggest structural differences between mature and immature CFTR.

Evidence for structural differences between WT CFTR and the processing mutant,  $\Delta$ F508, CFTR has also been obtained in other studies. Our results showing that the ER-trapped immature form of CFTR was more susceptible to protease digestion is in accordance with findings by Lukacs et al. (6). In their study, the kinetics, location, and inhibitor sensitivity of WT and  $\Delta$ F508 were examined. They showed that, in the early stages of biosynthesis, both WT and  $\Delta$ F508 were susceptible to degradation by endogenous protease, giving them half-lives of  $\sim 30$  min. While 45–80% of the WT protein was degraded in the ER, the rest became protease-resistant even if their progression to the Golgi was blocked by brefeldin A. Untreated  $\Delta$ F508, on the other hand, was not detected in the Golgi at all.

The mechanism of how processing defective mutations lead to the trapping and subsequent degradation of the CFTR protein is unclear. Some studies have suggested that the mislocalization of the CFTR processing-defective proteins is due to instability of the protein itself, leading to rapid degradation (6, 27). Studies using synthetic peptides, however, show processing-defective mutants, such as  $\Delta$ F508,

misfold locally and are trapped in an intermediate folding state while their stability remains unaffected (28–30). There is also evidence to suggest that molecular chaperones such as calnexin recognize the folding state of CFTR and show prolonged interaction with mutants that are defective in folding (31).

Recently, Johnston et al. (23) reported the discovery of a novel pericentriolar structure, the aggresome. In their study, they treated  $\Delta F508$ -expressing HEK 293 cells with a protease inhibitor, ALLN. The resultant immature  $\Delta F508$  CFTR was then shown to accumulate into a juxtanuclear cytosolic detergent-insoluble aggregate, an aggresome. The  $\Delta F508$  proteins were multiubiquitinated and deglycosylated. It was speculated that the protein was misfolded and was dislocated across the ER membrane by a Sec61p-dependent process and deglycosylated. Hence, it was concluded that the formation of aggresome was the result of a cellular response to misfolded proteins.

Our endo F digestion results, however, indicate that most of the WT CFTR protein trapped in an immature conformation by carrying out expression in COS-1 cells in the presence of MG-132 was still in the ER. Endo F is an amidase that cleaves off all sugar residues of high-mannose, hybrid, and complex oligosaccharides from N-linked glycoproteins such as CFTR. In Figure 3, there was an apparent reduction in molecular mass for MG-132-treated and untreated wild-type and  $\Delta F508$  CFTR after endo F digestion. Similar results were observed with Pgp. These results strongly suggest that the immature CFTR was still in the ER membrane. The discrepancy between our results and the results of Johnston et al. (23) may be due to differences in the cell lines used: COS-1 cells were used in the present study, while HEK 293 cells were used in the study by Johnston et al. (23). We have found that the effects of protease inhibitors on protein maturation differ in the two cell lines. In COS-1 cells, only MG-132 can block maturation of wild-type CFTR (Figure 3) or Pgp (unpublished results), while lactacystin and ALLN had no effect. In HEK 293 cells, however, both MG-132 and lactacystin could block maturation of wild-type CFTR (unpublished results) or Pgp (32).

Several lines of evidence indicate  $\Delta F508$  to be functional when it can be induced to mature and migrate to the cell surface upon expression at reduced temperature. It is functionally expressed on the cell surface of Sf9 (insect) cells (33) and *Xenopus* oocytes (34) where the cells are typically maintained at room temperature. Furthermore, the same functionality was shown for rescued  $\Delta F508$  CFTR at the mammalian cell surface by carrying out expression at lowered temperature (10) or in the presence of osmolytes such as glycerol (8) and dimethyl sulfoxide (9).

To date, only one group has shown channel activity for immature CFTR expressed in mammalian cells at 37 °C. Pasyk and Foskett (35) observed CFTR-like channel activity for  $\Delta F508$  in their patch clamp studies on the outer nuclear membrane (equivalent to the ER membrane) of CFTR- $\Delta F508$  stably transfected CHO cells. By contrast, we were unable to detect channel activity for immature CFTR.

There are several possible explanations for the discrepancy. (1) The structure of the immature CFTRs might not allow them to be incorporated into the lipid bilayer, hence no activity could be detected. (2) Pretreatment of their cells with sodium butyrate to increase  $\Delta F508$  expression might have

induced some the  $\Delta F508$  protein to mature and progress to the plasma membrane in a mature form (35). Butyrate has been shown to induce  $\Delta F508$  to the cell surface by overexpression (36, 37). Thus, what they were detecting might not have been the immature  $\Delta F508$  normally present at the ER membrane but mature CFTR. (3) The cell lines used for the two experiments might have different ER quality control systems. Thus, immature CFTR in CHO cells might be active, but immature CFTR in HEK 293 cells might not be. Iodide efflux assays done on  $\Delta F508$  stably transfected CHO cells have shown low but detectable CFTR-like channel activity (33). The iodide efflux assay is an alternative functional assay for CFTR proteins expressed on the cell surface. An inability to detect channel activity for  $\Delta F508$  CFTR expressed at 37 °C has also been reported by Chang et al. (38). They reported that they have never been able to detect CFTR-like single channels for  $\Delta F508$  expressed in BHK cells after incorporation into planar lipid bilayers.

In a recent study, P-glycoprotein, CFTR's sister protein, was also shown to be trapped in an immature form by MG-132 (11). The resultant immature protein was found to be more trypsin-sensitive than mature Pgp, and its COOH-histidine-tagged form also showed decreased affinity for the nickel resin. In the study, the immature Pgp was inactive when assayed for its ATPase activity. Our endo F digestion study shows that the immature protein is still in the ER membrane and not in an aggregate in the cytosol. Although immature Pgp or Pgp processing mutants were inactive, they could be converted to an active state by carrying out expression in the presence of drug substrates (18).

Recent research on CF has been focused on finding a cure for CF. Although processing mutants such as  $\Delta F508$  can be induced to reach the cell surface in vitro by expression at low temperature or in the presence of osmolytes such as glycerol and DMSO, these strategies are impractical for therapeutic uses. Thus, the goal is to find a drug that would induce the expression of these mutants to the cell surface without causing other side effects. Recent studies on rescuing other proteins with processing defects are encouraging to our efforts on finding a drug to achieve this goal. In Pgp, processing-defective proteins can be rescued by carrying out expression in the presence of drug substrates of Pgp (18). The antiarrhythmic drug E-4031, which selectively blocks HERG potassium channels, was also found to correct defective protein trafficking of the HERG potassium channels (39). Pgp, which shows maturation properties very similar to those of CFTR, can serve as a model for our search for a therapeutic drug to rescue mutant CFTRs whose maturation is impeded.

## ACKNOWLEDGMENT

We thank Dr. Tip W. Loo for placing the A52-histidine tag at the end of the CFTR cDNA and for technical support. We are grateful to Dr. David H. MacLennan for lending us the use of the planar lipid bilayer setup and the A52 epitope and antibody. The M3A7 antibody was a gift from Dr. John R. Riordan. The pMT21 expression vector was a gift from Dr. Randal Kaufman (Boston, MA).

## REFERENCES

1. Riordan, J. R., Rommens, J. M., Kerem, B., Alon, N., Rozmahel, R., Grzelczak, Z., Zielenski, J., Lok, S., Plavsic, N., Chou, J. L., et al. (1989) *Science* 245, 1066–1073.



2. Wine, J. J. (1999) *J. Clin. Invest.* 103, 309–312.
3. Seibert, F. S., Linsdell, P., Loo, T. W., Hanrahan, J. W., Riordan, J. R., and Clarke, D. M. (1996) *J. Biol. Chem.* 271, 27493–27499.
4. Seibert, F. S., Linsdell, P., Loo, T. W., Hanrahan, J. W., Clarke, D. M., and Riordan, J. R. (1996) *J. Biol. Chem.* 271, 15139–15145.
5. Seibert, F. S., Jia, Y., Mathews, C. J., Hanrahan, J. W., Riordan, J. R., Loo, T. W., and Clarke, D. M. (1997) *Biochemistry* 36, 11966–11974.
6. Lukacs, G. L., Mohamed, A., Kartner, N., Chang, X. B., Riordan, J. R., and Grinstein, S. (1994) *EMBO J.* 13, 6076–6086.
7. Ward, C. L., and Kopito, R. R. (1994) *J. Biol. Chem.* 269, 25710–25718.
8. Sato, S., Ward, C. L., Krouse, M. E., Wine, J. J., and Kopito, R. R. (1996) *J. Biol. Chem.* 271, 635–638.
9. Bebok, Z., Venglarik, C. J., Panczel, Z., Jilling, T., Kirk, K. L., and Sorscher, E. J. (1998) *Am. J. Physiol.* 275, C599–607.
10. Denning, G. M., Anderson, M. P., Amara, J. F., Marshall, J., Smith, A. E., and Welsh, M. J. (1992) *Nature* 358, 761–764.
11. Loo, T. W., and Clarke, D. M. (1999) *FASEB J.* 13, 1724–1732.
12. Rock, K. L., Gramm, C., Rothstein, L., Clark, K., Stein, R., Dick, L., Hwang, D., and Goldberg, A. L. (1994) *Cell* 78, 761–771.
13. Palombella, V. J., Rando, O. J., Goldberg, A. L., and Maniatis, T. (1994) *Cell* 78, 773–785.
14. Jensen, T. J., Loo, M. A., Pind, S., Williams, D. B., Goldberg, A. L., and Riordan, J. R. (1995) *Cell* 83, 129–135.
15. Zubrzycka-Gaarn, E., MacDonald, G., Phillips, L., Jorgensen, A. O., and MacLennan, D. H. (1984) *J. Bioenerg. Biomembr.* 16, 441–464.
16. Chen, C., and Okayama, H. (1987) *Mol. Cell Biol.* 7, 2745–2752.
17. Kartner, N., and Riordan, J. R. (1998) *Methods Enzymol.* 292, 629–652.
18. Loo, T. W., and Clarke, D. M. (1998) *J. Biol. Chem.* 273, 14671–14674.
19. Laemmli, U. K. (1970) *Nature* 227, 680–685.
20. Loo, T. W., and Clarke, D. M. (1995) *J. Biol. Chem.* 270, 21449–21452.
21. Tao, T., Xie, J., Drumm, M. L., Zhao, J., Davis, P. B., and Ma, J. (1996) *Biophys. J.* 70, 743–753.
22. Ward, C. L., Omura, S., and Kopito, R. R. (1995) *Cell* 83, 121–127.
23. Johnston, J. A., Ward, C. L., and Kopito, R. R. (1998) *J. Cell Biol.* 143, 1883–1898.
24. Wiertz, E. J., Tortorella, D., Bogoy, M., Yu, J., Mothes, W., Jones, T. R., Rapoport, T. A., and Ploegh, H. L. (1996) *Nature* 384, 432–438.
25. Plemper, R. K., Bohmler, S., Bordallo, J., Sommer, T., and Wolf, D. H. (1997) *Nature* 388, 891–895.
26. Zhang, F., Kartner, N., and Lukacs, G. L. (1998) *Nat. Struct. Biol.* 5, 180–183.
27. Lukacs, G. L., Chang, X. B., Bear, C., Kartner, N., Mohamed, A., Riordan, J. R., and Grinstein, S. (1993) *J. Biol. Chem.* 268, 21592–21598.
28. Thomas, P. J., Ko, Y. H., and Pedersen, P. L. (1992) *FEBS Lett.* 312, 7–9.
29. Qu, B. H., and Thomas, P. J. (1996) *J. Biol. Chem.* 271, 7261–7264.
30. Qu, B. H., Strickland, E. H., and Thomas, P. J. (1997) *J. Biol. Chem.* 272, 15739–15744.
31. Pind, S., Riordan, J. R., and Williams, D. B. (1994) *J. Biol. Chem.* 269, 12784–12788.
32. Loo, T. W., and Clarke, D. M. (1998) *J. Biol. Chem.* 273, 32373–32376.
33. Li, C., Ramjeesingh, M., Reyes, E., Jensen, T., Chang, X., Rommens, J. M., and Bear, C. E. (1993) *Nat. Genet.* 3, 311–316.
34. Drumm, M. L., Wilkinson, D. J., Smit, L. S., Worrell, R. T., Strong, T. V., Frizzell, R. A., Dawson, D. C., and Collins, F. S. (1991) *Science* 254, 1797–1799.
35. Pasyk, E. A., and Foskett, J. K. (1995) *J. Biol. Chem.* 270, 12347–12350.
36. Moyer, B. D., Loffing-Cueni, D., Loffing, J., Reynolds, D., and Stanton, B. A. (1999) *Am. J. Physiol.* 277, F271–276.
37. Cheng, S. H., Fang, S. L., Zabner, J., Marshall, J., Piraino, S., Schiavi, S. C., Jefferson, D. M., Welsh, M. J., and Smith, A. E. (1995) *Am. J. Physiol.* 268, L615–624.
38. Chang, X. B., Cui, L., Hou, Y. X., Jensen, T. J., Aleksandrov, A. A., Mengos, A., and Riordan, J. R. (1999) *Mol. Cell* 4, 137–142.
39. Zhou, Z., Gong, Q., and January, C. T. (1999) *J. Biol. Chem.* 274, 31123–31126.

BI992620M